Bioresource Technology 460 (2026) 135339

Contents lists available at ScienceDirect

Bioresource Technology

journal homepage: www.elsevier.com/locate/biortech

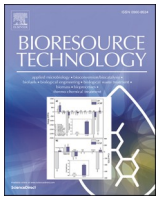

Tetraselmis chuii: Valorization of dairy wastewater using lactose as an alternative carbon source to glucose/galactose

Gloria Sciuto [a], Salim Kichouh-Aiadi [b], Yolanda Soriano-Jerez [b], Cinzia L. Randazzo [a], Nunziatina Russo [a], Cinzia Caggia [a,*], Maria del Carmen Cerón-García [b], Asterio Sánchez-Mirón [b]

[a] Department of Agriculture, Food and Environment, University of Catania, Via S. Sofia, 100, 95123, Catania, Italy
[b] Department of Chemical Engineering, University of Almería, Spain and CIAIMBITAL Research Centre, Almería, Spain

GRAPHICAL ABSTRACT

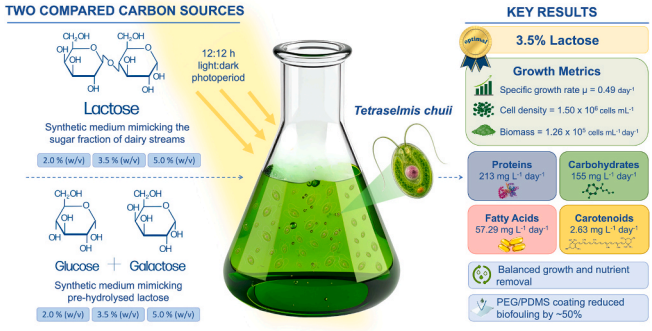

ARTICLE INFO

Keywords:
Tetraselmis chuii
Mixotrophy
Organic carbon source
Biochemical composition
Cell adhesion

ABSTRACT

This study evaluated the direct use of lactose, the main sugar fraction of dairy side-streams, for the mixotrophic cultivation of *Tetraselmis chuii*. An equimolar glucose/galactose mixture, representing the pre-hydrolysed equivalent of lactose, was included as a comparative treatment. Batch cultures were grown in synthetic media for 10 days at three carbon levels (2.0, 3.5, and 5.0 % w/v), using a photoautotrophic culture as a control. Growth performance, nutrient removal, biochemical productivities, and cell adhesion were assessed.

The 3.5 % lactose level showed the best overall performance, achieving a specific growth rate of 0.49 day^{-1}, a biomass productivity of 1.26×10^5 cells mL^{-1} day^{-1}, and a maximum cell density of 1.50×10^6 cells mL^{-1}. It also supported a balanced biomass composition, with protein, carbohydrate, fatty acid, and carotenoid productivities of 213, 154.71, 57.29, and 2.63 mg L^{-1} day^{-1}, respectively. In addition, under mixotrophic cultivation, PEG/PDMS coating reduced cell adhesion by approximately 50 % compared with glass.

These results highlight the potential of direct lactose use as a carbon source for the mixotrophic cultivation of *T. chuii*, supporting a sustainable strategy for the valorization of lactose-rich dairy by-products.

* Corresponding author.
E-mail address: cinzia.caggia@unict.it (C. Caggia).

https://doi.org/10.1016/j.biortech.2026.135339
Received 17 February 2026; Received in revised form 14 June 2026; Accepted 6 July 2026
Available online 7 July 2026

1. Introduction

The transition toward a circular bioeconomy requires innovative solutions that simultaneously address waste management and resource recovery. The dairy industry generates one of the most challenging agro-industrial waste streams: dairy wastewater (DWW), characterized by high organic loads, resulting in elevated values of chemical and biological oxygen demand (COD and BOD, respectively) (Zhao et al., 2020). DWW is a broad term that may refer to individual whey-derived streams, such as cheese whey (CW) and second cheese whey (SCW), as well as to mixed dairy effluents that may also include cleaning-in-place (CIP) waters. Consequently, its chemical composition and organic load can markedly vary depending on the stream composition and degree of mixing (Buchanan et al., 2023). In whey-derived streams, lactose is generally the predominant carbon source, about 2.0–7.0 % (w/v), together with residual proteins (about 0.1–0.2 % w/v), mineral salts (about 1–2 % w/v), and residual fats (about 0.1–0.6 % w/v) (Ozcelik et al., 2024; Sciuto et al., 2025). The discharge of improperly treated DWW into soil or natural water bodies can result in hypoxia or anoxia driven by uncontrolled microbial growth. Moreover, depending on the production process, DWW may contain excessive concentrations of nitrogen and phosphorus, potentially leading to eutrophication and further deterioration of water quality and aquatic ecosystems (Prazeres et al., 2012; Zhao et al., 2020).

Conventional DWW management relies on treatment processes that, although effective, are costly and generate secondary sludge, thus representing additional environmental challenges (Pires et al., 2021; Mahdavi and Tavakoli, 2025; Sciuto et al., 2025). Consequently, attention has shifted toward valorization strategies aligned with green chemistry and circular economy principles (Pires et al., 2021; Omran and Baek, 2022). Innovative approaches include bioenergy production, extraction of high-value biomolecules, and development of green nanomaterials, though these technologies still face challenges related to economic viability and technical scalability (Ryan and Walsh, 2016; Zhao et al., 2020; Pires et al., 2021; Mercado et al., 2020). Biological approaches have been proven as particularly promising for removing nitrate, phosphate, and contaminants through biosorption, bioaccumulation, biodegradation, and photodegradation (Gondi et al., 2022; Kiani et al., 2023; Occhipinti et al., 2025). Among biological remediation approaches, microalgae-based systems have emerged as particularly promising due to their dual functionality: simultaneous phytoremediation treatment and production of valuable biomass (Bhatnagar et al. 2011; Shahid et al., 2020; Das et al., 2022; La Bella et al., 2023; Occhipinti et al., 2023). Within microalgal cultivation strategies in agri-food residues, mixotrophic growth has proven particularly effective, as it enables the simultaneous utilization of light energy and dissolved organic carbon present in wastewater (Choi, 2016; Casagli et al., 2021). In several microalgal systems, supplementation with organic carbon sources has been associated with significant reductions in organic load, together with increases in growth and accumulation of reserve compounds (Macedo et al., 2015; Alkhamis et al., 2016; Heifetz et al., 2000; Sánchez-Zurano et al., 2024). In whey-based substrates, mixotrophic cultivation has also been shown to support higher biomass production, which is characterized by the accumulation of nutritionally relevant compounds such as proteins, lipids, and pigments (Pereira et al., 2019; Ozcelik et al., 2024). Beyond biomass productivity, biofouling represents an important operational challenge in large-scale microalgal cultivation systems, because cell adhesion in suspended photobioreactors can promote surface fouling, limit light penetration, and reduce process efficiency. This issue may be particularly relevant under mixotrophic conditions, where organic substrates can modify cell physiology, extracellular polymeric substance (EPS) secretion, and cell-surface physicochemical properties, thereby affecting adhesion behaviour (Zeriouh et al., 2017). In this context, antifouling materials such as PEG/PDMS-based coatings, including DBE-311-containing formulations, deserve attention as potential strategies to limit adhesion under realistic cultivation conditions (Soriano-Jerez et al., 2024; Conlon and Touzet, 2025).

Although lactose is the major organic component of whey-derived dairy effluents and is widely available as an inexpensive industrial by-product, its application as a carbon source for microalgal cultivation has received comparatively limited attention. In contrast, most existing studies have employed refined substrates, such as glucose or acetate, whose production and use involve additional processing steps and economic costs. The direct exploitation of lactose may therefore offer a more sustainable and economically attractive approach for large-scale microalgal cultivation.

Tetraselmis chuii is a mixotrophic microalga recently approved as a novel food by the European Commission. It has been widely investigated for its metabolic flexibility and high nutritional value (Rahman et al., 2017; Villar-Navarro et al., 2022). Its biomass is rich in proteins, digestible carbohydrates, and photosynthetic pigments, including chlorophylls and carotenoids, such as neoxanthin, violaxanthin, zeaxanthin, and α- and β-carotene. These compounds confer anti-stress and immunomodulatory effects (Majchrzak et al., 2025), making T. chuii widely used in aquaculture (Pereira et al., 2019; Muller-Feuga et al., 2003; Sciuto et al., 2025). The species tolerates wide ranges of salinity, temperature, and pH, making it suitable for wastewater-based cultivation systems (Malavasi et al., 2020; Hyung et al., 2021; Hosseini et al., 2022). Under mixotrophic conditions, *T. chuii* has shown up to fivefold higher productivity than autotrophic cultures, mainly using simple sugars such as glucose or acetate, with co-cultivation further enhancing performance (Han et al., 2016; Lu et al., 2017; Nzayisenga et al., 2018; Conlon et al., 2024). However, the ability of *T. chuii* to utilize lactose, a major carbon source in dairy wastewater, remains poorly explored.

The present study addresses this critical knowledge gap by investigating, for the first time, the ability of *T. chuii* to utilize lactose as the primary carbon source for mixotrophic cultivation, without prior hydrolysis, a step that has received limited attention to date. The direct use of lactose, rather than pre-hydrolyzed glucose/galactose mixtures, constitutes a significant simplification of the cultivation process, with the potential to reduce operational costs and facilitate the direct integration of microalgal production systems with lactose-rich dairy by-products. Although real dairy wastewater was not directly employed in the present study, the investigation focused on lactose, the principal organic component of whey-derived dairy effluents, as a representative substrate. This approach was intended to provide a preliminary assessment of the feasibility of utilizing lactose-rich dairy side streams for microalgal cultivation and to support the development of simplified, scalable, and industrially relevant bioprocesses for their valorization. The effects of lactose on growth dynamics, nitrogen and phosphorus removal efficiency, and biomolecule accumulation were systematically compared with those of equimolar glucose/galactose mixtures at equivalent carbon concentrations.

2. Materials and methods

2.1. Microalgal culture

T. chuii, provided by INMAR (University of Cádiz, Spain), was grown in photoautotrophic cultivation in 1-L spherical flasks aerated with atmospheric air and maintained in *N*-optimized ALGAL (*N*-ALGAL) medium (Camacho-Rodríguez et al., 2015). The composition of the final medium was as follows (g L^{-1}): KNO_3, 1.13; $NaH_2PO_4{\cdot}H_2O$, 0.076; $C_6H_8FeO_7{\cdot}H_2O$, 0.015; $Na_2MoO_4{\cdot}2H_2O$, 0.0016; $MnCl_2{\cdot}4H_2O$, 0.0012; $ZnCl_2$, 0.0009; $CoCl_2{\cdot}6H_2O$, 0.00014; $CuSO_4{\cdot}5H_2O$, 0.00021; EDTA, 0.015; vitamin B1, 0.003; B7, 3.8×10^{-5}; and vitamin B12, 2.7×10^{-5}.

2.2. Culture conditions

All *T. chuii* cultures used in this study were non-axenic; before the experiment, they were maintained under standard photoautotrophic

conditions. No antibiotic treatment or sterilization of the inoculum was performed, and the associated bacterial microbiota was not eliminated. Triplicate mixotrophic cultures of *T. chuii* were grown in 250-mL Erlenmeyer flasks containing 100 mL of *N*-ALGAL medium. Lactose was added at final concentrations of 2.0, 3.5, and 5.0 % (w/v), hereafter referred to as L2 %, L3.5 %, and L5 %, respectively, to reproduce the lactose levels commonly found in dairy by-products and wastewaters (Pires et al., 2021; Sciuto et al., 2025). To simulate complete lactose hydrolysis and assess direct monosaccharide utilization (Lu et al., 2017), cultures of *T. chuii* were supplemented with an equimolar glucose/galactose mixture at the same final concentrations, hereafter designated as Glu/Ga2 %, Glu/Ga3.5 %, and Glu/Ga5 %. The two treatments, Lactose and Glu/Ga, were prepared separately in *N*-ALGAL medium, with each condition containing only lactose or only Glu/Ga as the added carbon source. Ready-to-use powdered lactose, glucose, and galactose were obtained from Sigma-Aldrich (St. Louis, MO, USA). For all treatments, the pH of the medium was approximately adjusted to 7.0 before inoculation. Cultures were inoculated at the same initial cell concentration (of approximately 2.0 x 10^5 cell mL^{-1}) and incubated for 10 days under orbital shaking (180 rpm) at 24 ± 1 °C under a 12:12 h light:dark photoperiod, with an incident photon flux density of 130 ± 10 μmol photons m^{-2} s^{-1}. Triplicate phototrophic cultures grown in *N*-ALGAL medium without carbohydrate supplementation served as the phototrophic control (PC).

2.3. Growth performance

Growth performance was monitored every two days by flow cytometry (CytoFLEX LX, Beckman Coulter) in culture aliquots. Measured parameters included cell concentration (events mL^{-1}), cell size estimated from forward scatter (FSC) calibrated against size-reference beads, cellular granularity from side scatter (SSC) as an indicator of physiological state, and chlorophyll-a autofluorescence (excitation 488 nm, emission 690 nm; B690/PC5.5 channel). The cytometer was calibrated with fluorescent beads before each analytical run to ensure measurement consistency across experiments. The physiological state was additionally evaluated every two days by determining *Fv/Fm* with a PAM-2500 chlorophyll fluorometer (Heinz Walz GmbH). The pH was also recorded every two days and corrected to neutrality by adding NaOH if necessary.

Cell weight (*CW*, pg $cell^{-1}$) was calculated by correlating dry weight (*DW*, g L^{-1}) with cell concentration (*C*, cells mL^{-1}) at different times of culture and with the different culture conditions (Minio et al., 2025). Dry weight was determined by filtering 10-mL culture aliquots in pre-weighed tubes, rinsing with 0.5 M ammonium bicarbonate to remove residual salts, freeze-drying, and reweighing. The cell weight was then calculated according to the following equation:

$$CW = \frac{DW}{C} \bullet 10^6 \quad (1)$$

2.4. Growth kinetics

The maximum specific growth rate μ (day^{-1}) was determined during the exponential phase by dividing the slope of the biomass concentration profile by the average biomass concentration (Levasseur et al., 1993):

$$\mu = \frac{1}{C}\frac{dC}{dt} = \frac{lnC - lnC^0}{t - t^0} \quad (2)$$

Where *C* is the cell concentration at each time (t, days) and C^0 is the cell concentration at the initial time (t^0, days). Final biomass productivity (P_B, cell mL^{-1} day^{-1}) was calculated as the difference between final and initial biomass concentrations divided by the cultivation time in days:

$$P_B = \frac{C - C^0}{t - t^0} \quad (3)$$

2.5. Growth monitoring

Nutrient consumption was assessed by comparing nitrate, phosphate, and total carbohydrate (TC) concentrations in the culture supernatant collected at the beginning (day 0) and at the end of cultivation time (day 10). For this purpose, 2 mL of microalgae cultures were centrifuged at 7500 rpm for 5 min. An aliquot of the resulting supernatant was used for the determination of nitrate and phosphate concentrations, according to the American Public Health Association methods (APHA) 4500-N and 4500-P, respectively. TC was also determined in the supernatant by the anthrone–sulfuric acid colorimetric assay (Sim et al., 1997). In particular, 0.5 mL of supernatant was mixed with 1 mL of anthrone reagent in screw-cap glass tubes, placed in cold water (10–15 °C), vortexed, and incubated for 15 min at 100 °C. After cooling to room temperature for 1 h, absorbance was recorded at 625 nm in triplicate against a reagent blank. Carbohydrate concentration was calculated from a glucose calibration curve prepared from a 1 g L^{-1} stock; standards of 10–70 μg mL^{-1} were processed identically to the samples. For each parameter (nitrate, phosphate, and TC) measurements were carried out in triplicate, and the average value was calculated.

For biochemical composition analyses, biomass was harvested at the end of cultivation time (day 10) by centrifugation (Allegra 25R, Beckman Coulter) at 3000xg for 15 min in 50-mL Falcon tubes, then washed twice with 0.5 M ammonium bicarbonate solution (Zhu and Lee, 1997) and subsequently lyophilized using a vacuum freeze-dryer (Cryodos 50, Telstar). The dried biomass was frozen and stored at − 20 °C for further analysis.

2.6. Biochemical composition

2.6.1. Proteins

Protein content in dry biomass was determined as previously reported by Kichouh-Aiadi et al (2025). Lyophilized biomass (5 mg) was vortexed in 200 μL 24 % trichloroacetic acid (TCA), heated at 95 °C for 15 min in screw-capped tubes, cooled, and diluted to 6 % TCA with 600 μL water, and centrifuged (15,000 × g, 20 min, at 4 °C; Allegra 25R, Beckman Coulter). Pellets were resuspended in 0.5 mL Lowry Reagent D (A:B:C = 48:1:1; A: 2 % Na2CO3 in 0.1 N NaOH; B: 1 % NaK tartrate; C: 0.5 % CuSO4··5H2O), incubated at 55 °C for 30 min, cooled, and centrifuged (15,000 × g, 20 min, room temperature). Protein in the supernatant was quantified by bicinchoninic acid (BCA) assay at 562 nm using a microplate reader (Synergy Mx, BioTek).

Protein productivity at harvest (P_{PRT}) was calculated as:

$$P_{PRT} = P_B \bullet CW \bullet \%PRT \quad (4)$$

where P_B (cell mL^{-1} day^{-1}) is biomass productivity, *CW* (pg $cell^{-1}$) is the cell weight, and *%PRT* (% DW) is the protein content of dry biomass. All measurements were performed in three technical and biological replicates, and mean values were calculated.

2.6.2. Fatty acids

Freeze-dried microalgal biomass required no pretreatment for saponifiable lipid (SL) analysis. SLs were quantified by the reaction of transesterification of fatty acids (FA) to their methyl esters (FAME) by gas chromatography. Briefly, 10 mg of freeze-dried biomass were extracted with 1 mL of hexane, then 0.125 mg of nonadecanoic acid (C19:0) was added as an internal standard. Methylation was performed by adding 1 mL of acetyl chloride:methanol (1:20, v/v) to the hexane extract and heating for 20 min at 105 °C. After cooling to room temperature, 1 mL of water was added to induce phase separation, and the samples were centrifuged. Then, the upper hexane phase (containing FAME) was recovered into GC vials for analysis. FAMEs were analyzed by GC-FID Agilent Technologies 6890 N (Rodríguez-Ruiz et al.,1998; Kichouh-Aiadi et al., 2025). The chromatograph was equipped with a fused-silica OmegaWax™ capillary column (30 m × 0.25 mm i.d., 0.25

μm film; Supelco) and a flame ionization detector (FID). Nitrogen was used as carrier gas at 58.1 mL min^{-1} with a 1:40 split ratio; injector and detector temperatures were 250 and 260 °C, respectively. The oven program was: 150 °C for 3 min, ramp to 240 °C at 7.5 °C min^{-1}, and hold at 240 °C for 12 min. FAMEs were identified by retention-time comparison with the Long-chain FAME Mixture standard (Ref. 28663, Cayman Chemical), injected at the start and end of each sequence as QC.

Fatty acid productivity at harvest (P_{FA}) was calculated as:

$$P_{FA} = P_B \bullet CW \bullet \%FA \quad (5)$$

where P_B (cell mL^{-1} day^{-1}) is biomass productivity, CW (pg $cell^{-1}$) is the cell weight, and $\%FA$ (% DW) is the fatty acid content of dry biomass. All measurements were performed in triplicate, and mean values were calculated.

The relative percentages of saturated (SFA), monounsaturated (MUFA), and polyunsaturated (PUFA) fatty acids were calculated as the ratio of each fraction to the total fatty acid (TFA) content, expressed as percentages: %SFA = (ΣSFA / TFA) × 100; %MUFA = (ΣMUFA / TFA) × 100; %PUFA = (ΣPUFA / TFA) × 100, where ΣSFA, ΣMUFA, and ΣPUFA represent the sum of the saturated, monounsaturated, and polyunsaturated fatty acid concentrations, respectively, and TFA is the total fatty acid content of the sample.

2.6.3. Carotenoids

Carotenoids were extracted from 5 mg of dried biomass with 1 mL of a hexane:ethanol:water mixture (18:76:6) for 2 min at 25 °C without saponification (no KOH). Carotenoid concentrations in the extracts were quantified by HPLC with photodiode-array detection (Shimadzu SPDM10AV; Shimadzu Corp.), following the method previously described by Cerón-García and co-workers (2018). Separation was achieved on a LiChrospher© 100 RP-18 (5 μm, 4.6 × 150 mm) column using solvents A (water:methanol 1:4 v/v) and B (acetone:methanol 1:1 v/v) under a gradient from 25 to 100 % B over 32 min at a flow rate of 1 mL min^{-1}. Detection wavelengths were 440, 450, and 475 nm. Carotenoids were identified and quantified using calibration curves based on authentic standards (Sigma; DHI Lab Products).

Carotenoid productivity at harvest (P_{CRT}) was calculated as:

$$P_{CRT} = P_B \bullet CW \bullet \%CRT \quad (6)$$

where P_B (cell mL^{-1} day^{-1}) is biomass productivity, CW (pg $cell^{-1}$) is the cell weight, and $\%CRT$ (% DW) is the carotenoid content of dry biomass. All measurements were performed in triplicate, and mean values were calculated.

2.6.4. Total carbohydrates

Carbohydrates in the biomass were quantified by the anthrone–sulfuric acid colorimetric assay (Sim et al., 1997), following the same analytical procedure described in Section 2.5, with an additional preparative step required for dry biomass analysis. In particular, 2 mg of dry biomass were hydrolyzed in 2 mL of 1 N HCl for 2 h at 100 °C before colorimetric determination.

Carbohydrate productivity at harvest (P_{CAR}) was calculated as:

$$P_{CAR} = P_B \bullet CW \bullet \%CAR \quad (7)$$

where P_B (cell mL^{-1} day^{-1}) is biomass productivity, CW (pg $cell^{-1}$) is the cell weight, and $\%CAR$ (% DW) is the carbohydrate content of dry biomass. All measurements were performed in triplicate, and mean values were calculated.

2.7. Microalgae cell adhesion

T. chuii in mixotrophic cultures was also used as a tester to determine the antifouling efficiency of a novel transparent fouling-release coating. The coating was developed according to the protocol described by Soriano-Jerez and co-workers (2024). Briefly, a PEG/PDMS copolymer (DBE-311, Gelest) was added (4 % w/w) to the PDMS oil (Sylgard 184; PDMS: crosslinker 10:1 w/w). Xylene (<10 % w/w) was used as a solvent to facilitate mixing. To ensure a defect-free surface, the mixture was degassed under vacuum and subsequently applied onto borosilicate glass brackets (20x52 mm; Normax®). A micrometer film applicator (3580/3 Universal, Neurtek) was used to achieve a controlled thickness of 120 μm. Finally, the coatings were cured in an oven at 120 °C for 30 min to complete the crosslinking reaction. The coating and a borosilicate glass slide were placed at the bottom of the PBR. Cell adhesion was quantified at the end of the culture by measuring the chlorophyll-a fluorescence (Soriano-Jerez et al., 2021).

2.8. Statistical analysis

All data were analysed using GraphPad Prism version 10.0 (GraphPad Software). Experimental data from all treatments are presented as mean ± standard deviation (SD) calculated from independent biological replicates (n = 3). Comparisons among treatment groups were conducted using one-way analysis of variance (ANOVA) followed by Tukey's honest significant difference (HSD) post-hoc test for pairwise comparisons. Graphs and statistical outputs were generated directly from GraphPad Prism.

3. Results

3.1. Growth performance

Growth performance, photosynthetic activity, and pH dynamics are summarized in Fig. 1A, 1B, and 1C, respectively. At the end of cultivation duration (day 10), cell concentrations increased substantially under lactose supplementation ($p < 0.05$), compared to the photoautotrophic control (PC). Among all treatments, lactose at 3.5 % (L3.5 %) achieved the highest cell concentration (1.50 × 10^6 cells mL^{-1}). Under glucose/galactose (Glu/Ga) supplementation, the highest value was observed at day 10 in Glu/Ga 3.5 % (9.43 × 10^5 cells mL^{-1}), still higher than the control (7.87 × 10^5 cells mL^{-1}) but markedly lower than all lactose treatments. The improved performance observed in lactose-supplemented cultures may be associated with the slower dynamics of carbon availability, which likely alleviated metabolic stress and promoted the preservation of cellular physiological balance. A similar pattern of enhanced performance under lactose supplementation was observed for the photosynthetic efficiency (Fig. 1, panel B). Lactose cultures showed only a gradual initial decline and maintained measurable *Fv/Fm* values, remaining, after 10 days, between approximately 0.40 (L3.5 %) and 0.50 (L2 %). By contrast, glucose/galactose cultures exhibited a rapid decrease, mainly starting from the 4th day, significantly lower than values observed for both lactose and control cultures ($p < 0.05$). After 6 days, all glucose/galactose cultures converged to *Fv/Fm* values around 0.10. The pH profile followed the same pattern (Fig. 1, panel C). In lactose cultures, pH remained close to neutrality throughout cultivation, whereas in glucose/galactose cultures, it acidified rapidly by day 4 (around 6.5), showing significant differences compared with both the control and lactose ($p < 0.05$) and requiring repeated pH correction. In contrast, the control displayed progressive basification above pH 9.00.

For each treatment, the maximum specific growth rate (μ), biomass productivity (P_B), the percentages of nitrate and phosphate, and total carbohydrate (TC) reduction were determined. All mixotrophic treatments showed higher μ (0.49 day^{-1}), P_B (126,100 cell mL^{-1} day^{-1}), and nitrate removal (93 %) than the PC (μ = 0.27 day^{-1}; P_B = 54,650 cell mL^{-1} day^{-1}; nitrate removal 90.4 %). Phosphate removal was the only parameter that remained higher in the PC, around 84.8 %.

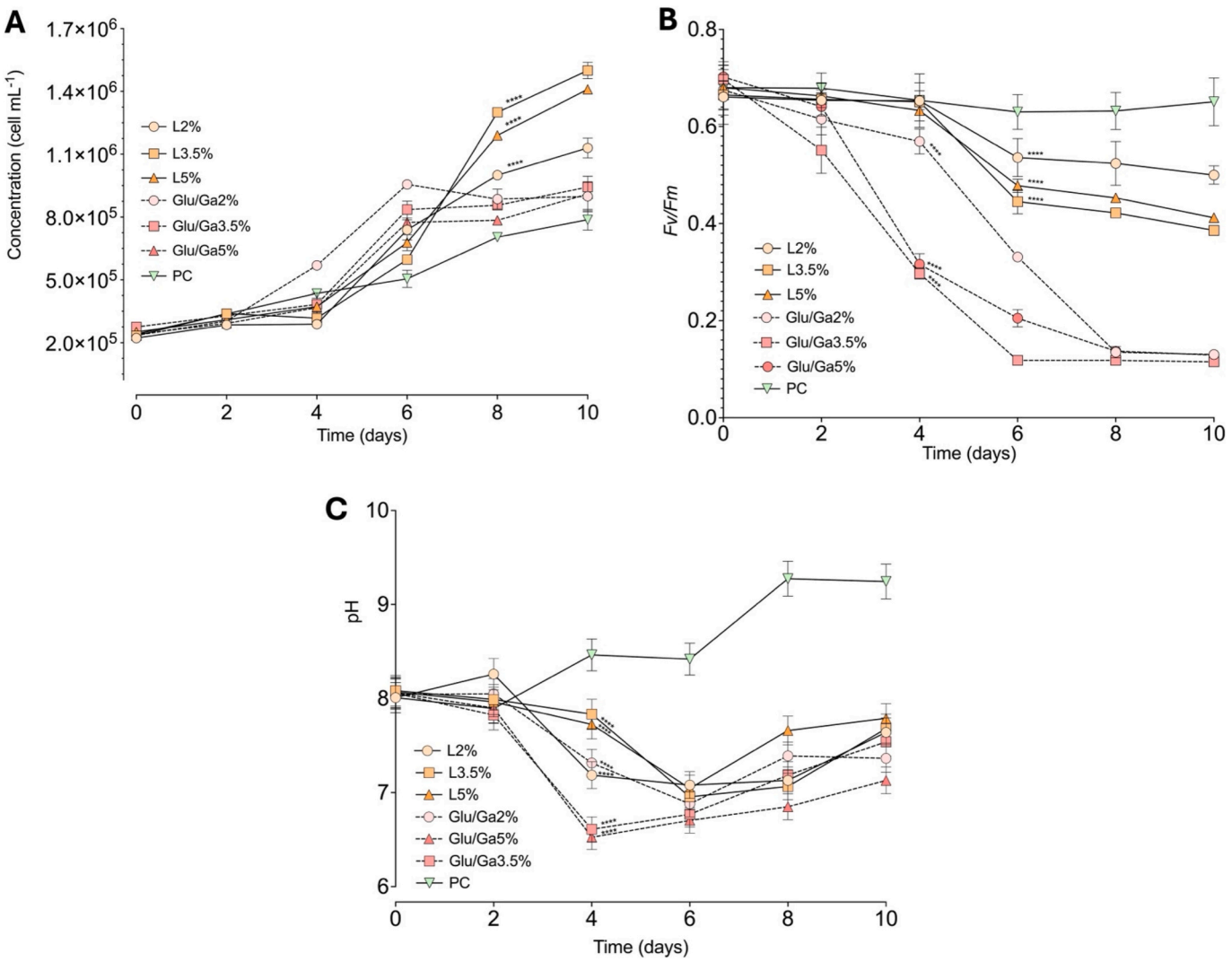

Fig. 1. Dynamics of (A) cell concentrations (cells mL^{-1}); (B) photosynthetic efficiency (*Fv/Fm*) and (C) pH in microalgal cultures grown mixotrophically with lactose (L2 %, L3.5 %, L5 %) or glucose/galactose (Glu/Ga2 %, Glu/Ga3.5 %, Glu/Ga5 %), compared with the photoautotrophic control (PC). Data are expressed as mean ± SD (n = 3). Significant differences compared to the control are indicated (**** $p < 0.0001$).

3.2. Effect of mixotrophy on morphology

Flow cytometry parameters included forward scatter (FSC, proxy for cell volume), side scatter (SSC, proxy for intracellular granularity and complexity), and chlorophyll-a autofluorescence (B690, proxy for photosynthetic capacity) (Fig. 2). Data were filtered using a B690 threshold of 10,000 to ensure analysis of photosynthetically active cells. FSC distributions showed substantial treatment-dependent variation in cell volume (Fig. 2-I A, B, C). Bimodal cell size distributions were observed in both lactose- and glucose/galactose-supplemented cultures. In lactose treatments, the two populations were centered at approximately 10 μm and 20 μm equivalent diameter, with L3.5 % exhibiting the most prominent larger-cell fraction. In contrast, glucose/galactose treatments showed a marked shift toward smaller cell sizes, with a substantial population below 3 μm equivalent diameter, while the larger fraction remained within the 10–20 μm range. The photoautotrophic control showed a single, homogeneous distribution around 10 μm. SSC analysis revealed distinct granularity patterns (Fig. 2-II A, B, C). Lactose treatments maintained moderate intensities, with L3.5 % and L5 % slightly higher compared to L2 %. Glucose/galactose cultures displayed substantially higher SSC values, particularly Glu/Ga2 % and Glu/Ga3.5 %, indicating considerable intracellular accumulation despite smaller cell sizes. The photoautotrophic control showed the lowest SSC intensity, consistent with reduced cellular complexity relative to carbon-supplemented cultures. Conversely, B690 fluorescence signals served as a proxy for the preservation of photosynthetic functionality (Fig. 2-III A–C). The smaller cell size in glucose/galactose cultures is consistent with metabolic stress induced by rapid substrate utilization and associated acidification, which likely impaired cell expansion and division. Lactose cultures retained robust chlorophyll-a fluorescence (L2 % > L3.5 % > L5 %), while glucose/galactose treatments showed severely diminished intensity by day 10, with Glu/Ga3.5 % and Glu/Ga5 % exhibiting near-complete loss of photosynthetic machinery. The photoautotrophic control maintained a moderate B690 fluorescence intensity, comparable to that observed in lactose-supplemented cultures.

3.3. Biochemical composition under mixotrophic conditions

Protein content in mixotrophic cultures is shown in Fig. 3A. In lactose media, protein content ranged from 1.38 ng $cell^{-1}$ in L2 % to 1.84 ng $cell^{-1}$ in L5 %. The increase observed at L5 % was statistically significant compared to L2 % and L3.5 % ($p < 0.05$). In glucose/galactose media, protein values varied significantly between 1.48 ng $cell^{-1}$ in Glu/Ga5 % and 1.71 ng $cell^{-1}$ in Glu/Ga 3.5 % ($p < 0.05$). All mixotrophic treatments, both lactose and glucose/galactose, exhibited protein contents significantly higher than the photoautotrophic control (p

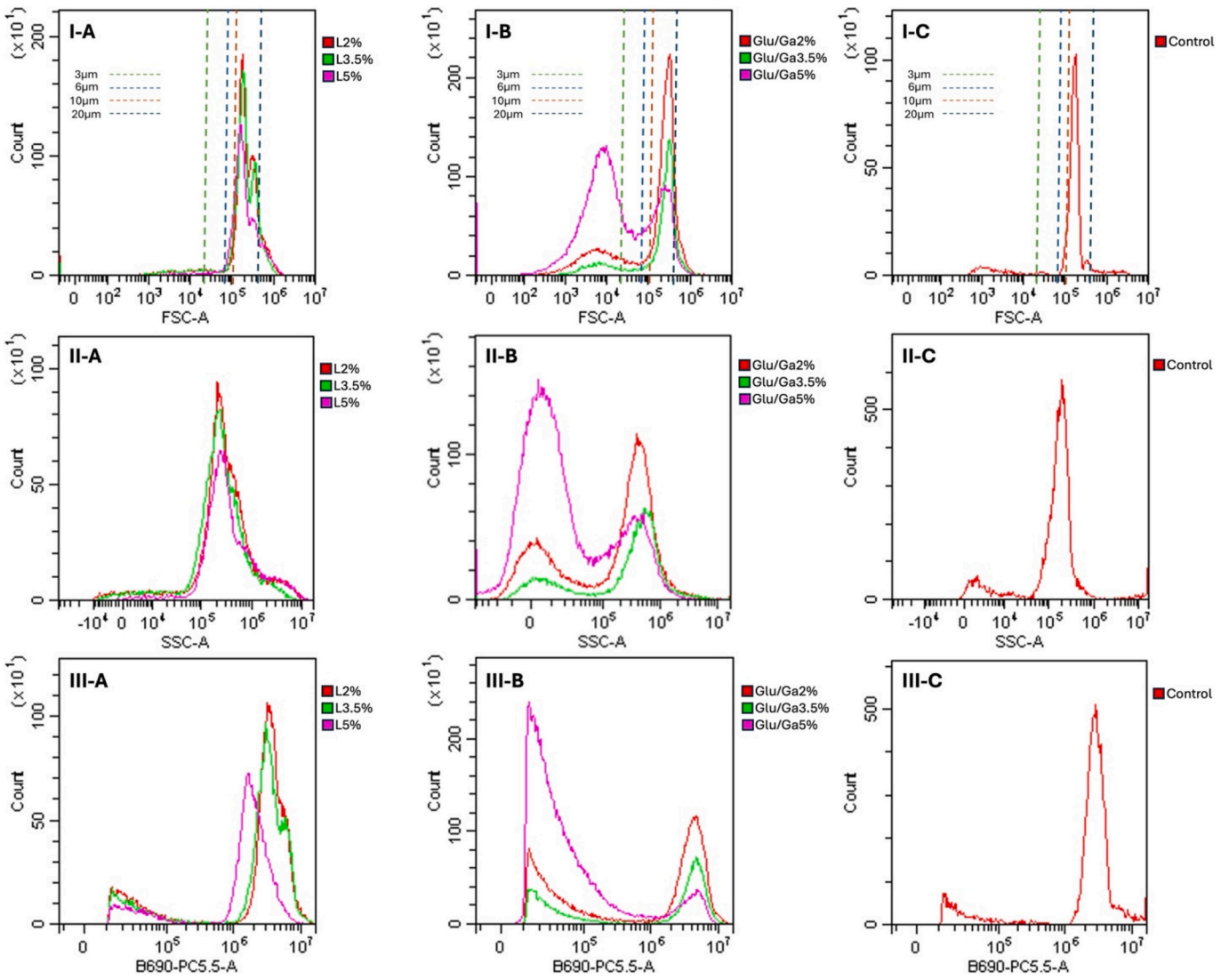

Fig. 2. FSC, SSC, and B690 histograms (I, II, and III, respectively) at day 10 with size beads calibration standards (3, 6, 10, 20 µm). Lactose trials (A), glucose/galactose (B), and photoautotrophic control PC (C).

< 0.05), which recorded 0.31 ng cell^{-1}. Overall, the highest protein content was detected in L5 %, which was significantly greater than all other conditions ($p < 0.05$). The higher protein content in L5 % may reflect enhanced nitrogen assimilation driven by greater metabolic activity, consistent with a balanced mixotrophic regime.

The total fatty acid content and its composition in terms of saturated fatty acids (SFA), monounsaturated fatty acids (MUFA), and polyunsaturated fatty acids (PUFA) are shown in Fig. 3B. In lactose-based media, total fatty acids ranged from 0.43 to 0.46 ng cell^{-1}, with PUFA ranging from 0.15 to 0.14 ng cell^{-1}. These values did not differ significantly among lactose concentrations, while all were higher than the control ($p < 0.05$). In glucose/galactose media, total fatty acid content was higher and increased with substrate concentration, ranging from 0.58 ng cell^{-1} to 0.95 ng cell^{-1}, with PUFA ranging from 0.14 to 0.26 ng cell^{-1}. The increase observed in Glu/Ga5 % was statistically significant compared to all lactose treatments and to the control ($p < 0.05$). The photoautotrophic control showed the lowest lipid accumulation, with 0.15 ng cell^{-1} total fatty acids, and 0.04 ng cell^{-1} PUFA. The enrichment in PUFA under glucose/galactose conditions, particularly in Glu/Ga5 %, may be nutritionally relevant given the role of ω-3 and ω-6 fatty acids in aquaculture feed and functional food formulations.

Carbohydrate content in mixotrophic cultures is presented in Fig. 3C. In lactose-based media, values ranged from 1.18 ng cell^{-}1 in L2 % to 1.25 ng cell^{-}1 in L5 %. In glucose/galactose media, carbohydrate levels were significantly higher than in lactose treatments ($p < 0.05$), reaching 1.90 ng cell^{-}1 in Glu/Ga2 %, 1.79 ng cell^{-}1 in Glu/Ga3.5 %. All mixotrophic cultures showed significantly higher ($p < 0.05$) carbohydrate contents compared to the photoautotrophic control (0.29 ng cell^{-}1). The highest carbohydrate accumulation was detected in the Glu/Ga2 % treatment, with values significantly exceeding those observed in all other experimental conditions ($p < 0.05$). In addition to macromolecular fractions, the photosynthetic pigment content was analysed to assess the effect of the carbon source on the cells' light-harvesting capacity. The carotenoid content (Fig. 3D) was highest (22 pg cell^{-}1) in L2 %. In glucose/galactose, the carotenoid content values were approximately 13.43 pg cell^{-}1 in Glu/Ga2 %, and 12.42 pg cell^{-}1 in Glu/Ga5 %. The photoautotrophic control (PC) showed a carotenoid content of 22.99 pg cell^{-}1. Carotenoid content did not differ significantly among lactose concentrations ($p > 0.05$); however, all lactose treatments showed significantly higher carotenoid levels than glucose/galactose cultures ($p < 0.05$). All Glu/Ga treatments showed significantly lower carotenoid levels compared to both the lactose media and the control ($p < 0.05$).

Chlorophyll content followed a pattern analogous to that of carotenoids (Fig. 3E). Lactose treatments maintained significantly higher chlorophyll levels (up to 31 pg cell^{-1} in L2 %) than glucose/galactose

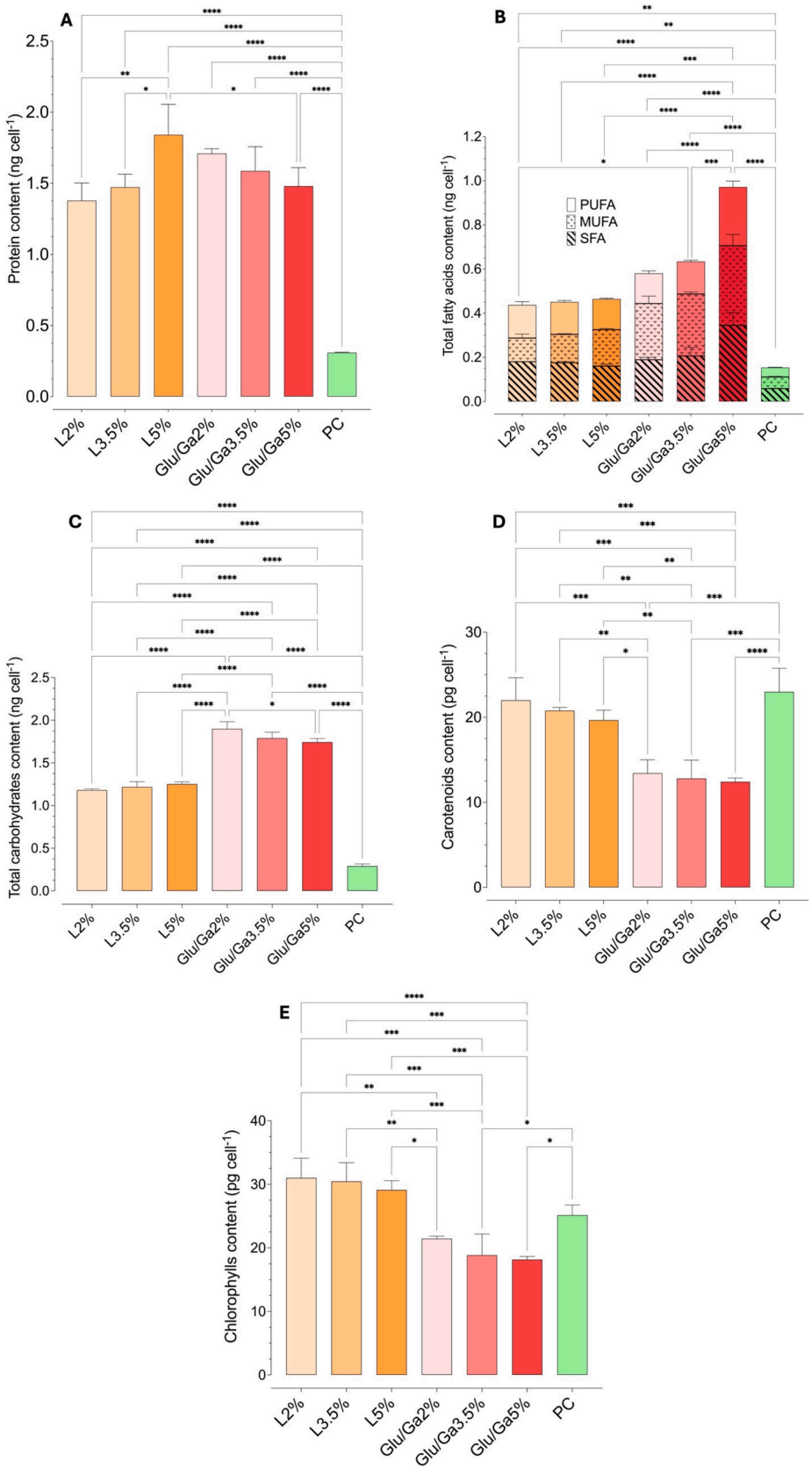

Fig. 3. Protein (A) content (ng cell^{-1}), Total fatty acid (B) content (ng cell^{-1}) and composition (SFA, MUFA, PUFA), Total carbohydrates (C) content (ng cell^{-1}), Carotenoid (D) content (ng cell^{-1}) and Chlorophyl (E) content (pg cell^{-1}) in mixotrophic cultures grown with different concentrations of lactose (L2 %, L3.5 %, L5 %) and glucose/galactose (Glu/Ga2 %, Glu/Ga3.5 %, Glu/Ga5 %), and the photoautotrophic control (PC). Data are expressed as mean ± SD (n = 3). Significant differences between treatments are indicated (* $p < 0.05$, ** $p < 0.01$, *** $p < 0.001$, **** $p < 0.0001$).

cultures (max. 21.44 pg cell^{-1}) and, in the case of Glu/Ga, also lower than the photoautotrophic control (25.15 pg cell^{-1}; $p < 0.05$). No significant differences were detected among lactose concentrations.

3.4. Macromolecular productivity

Volumetric productivities of macromolecular fractions (mg L^{-1} day^{-1}) for all treatments are shown in Fig. 4A (proteins, carbohydrates, and fatty acid productivity) and 4B (carotenoid productivity). Overall, the highest productivity was 213 mg L^{-1} day^{-1} for protein in L5 % and 154.71 mg L^{-1} day^{-1} for carbohydrate in L3.5 %. In all the treatments, the maximum fatty acid productivity was 65.10 mg L^{-1} day^{-1} in Glu/Ga5 %. The maximum carotenoid productivity, 2.63 mg L^{-1} day^{-1}, was reached in L3.5 %. In PC, protein, carbohydrate, and fatty acid productivities were markedly lower, with values of 16.89, 15.92, and 8.42 mg L^{-1} day^{-1}, respectively, while carotenoid production was 1.26 mg L^{-1} day^{-1}. The higher protein productivity in L5 % (213 mg L^{-1} day^{-1}) compared to lower lactose concentrations is consistent with increased nitrogen assimilation at higher carbon availability, where a balanced C:N ratio promotes amino acid synthesis rather than carbon storage. The fact that L3.5 %, rather than L5 %, maximized carbohydrate productivity (154.71 mg L^{-1} day^{-1}) suggests that at higher lactose concentrations, carbon flux may be partially redirected toward protein synthesis, reflecting the metabolic flexibility of *T. chuii* under mixotrophic conditions. In glucose/galactose cultures, the dominance of fatty acid productivity in Glu/Ga5 % (65.10 mg L^{-1} day^{-1}) is consistent with the carbon-overflow mechanism, whereby excess readily available monosaccharides are channelled into lipid storage. The high carotenoid productivity in lactose conditions (up to 2.63 mg L^{-1} day^{-1} in L3.5 %) is directly linked to the maintenance of photosynthetic activity observed in these cultures. Compared to the PC, L3.5 % achieved approximately 13-fold higher protein, 10-fold higher carbohydrate, 7-fold higher fatty acid, and 2-fold higher carotenoid productivities.

3.5. Cell adhesion

Fig. 5 illustrates the influence of lactose (Fig. 5A) and Glu/Ga (Fig. 5B) concentrations on biomass production, cell adhesion on glass coating surfaces, and biomass composition. In both culture systems, cell adhesion depended on medium composition and surface type. Adhesion on the PEG/PDMS coating was significantly lower than on glass under all tested conditions ($p < 0.05$), confirming its antifouling performance in mixotrophic cultures.

On glass, cell adhesion was highest in the photosynthetic controls and decreased with increasing lactose or Glu/Ga concentration, stabilizing at lower levels at intermediate substrate concentrations. Although adhesion trends were similar for both carbon sources, slightly higher adhesion values were observed in lactose cultures, particularly under photosynthetic controls. Conversely, adhesion on the coating remained low and comparable across all treatments, indicating a stable antifouling response regardless of medium composition.

4. Discussion

4.1. Growth and physiological response

The key outcome of the present study is that *T. chuii* showed higher growth when cultivated on lactose than on glucose/galactose mixtures. The best performance was observed at 3.5 % (w/v) lactose, supporting the feasibility of lactose-based mixotrophic cultivation with direct relevance to lactose-rich dairy wastewater streams. Collectively, these results indicate that the contrasting responses observed under lactose and glucose/galactose supplementation cannot be explained solely by differences in carbon availability. Rather, they appear to be strongly influenced by the molecular form of the carbon source and the associated patterns of uptake and metabolism within the culture system. Similar positive responses to lactose-based mixotrophic cultivation have also been reported in selected microalgal species, including *Graesiella emersonii* and *Parachlorella kessleri*, while *Chlorella vulgaris* has also shown improved growth under cheese whey/lactose supplementation (de Andrade et al., 2022; Hidasi et al., 2024; Kolesovs et al., 2025). Overall, these studies and our results indicate that the ability to exploit lactose is strongly species-dependent and often requires specific cultivation conditions. Some studies have related lactose utilization to β-galactosidase activity in microalgae (do Amaral Santos et al., 2021; Kolesovs et al., 2025), whereas others have suggested that associated bacteria may also contribute to lactose conversion in non-axenic systems (Sial et al., 2021). In the present study, although the experiments were performed under sterile conditions, the starting *T. chuii* culture was not axenic, and neither β-galactosidase activity nor bacterial contribution

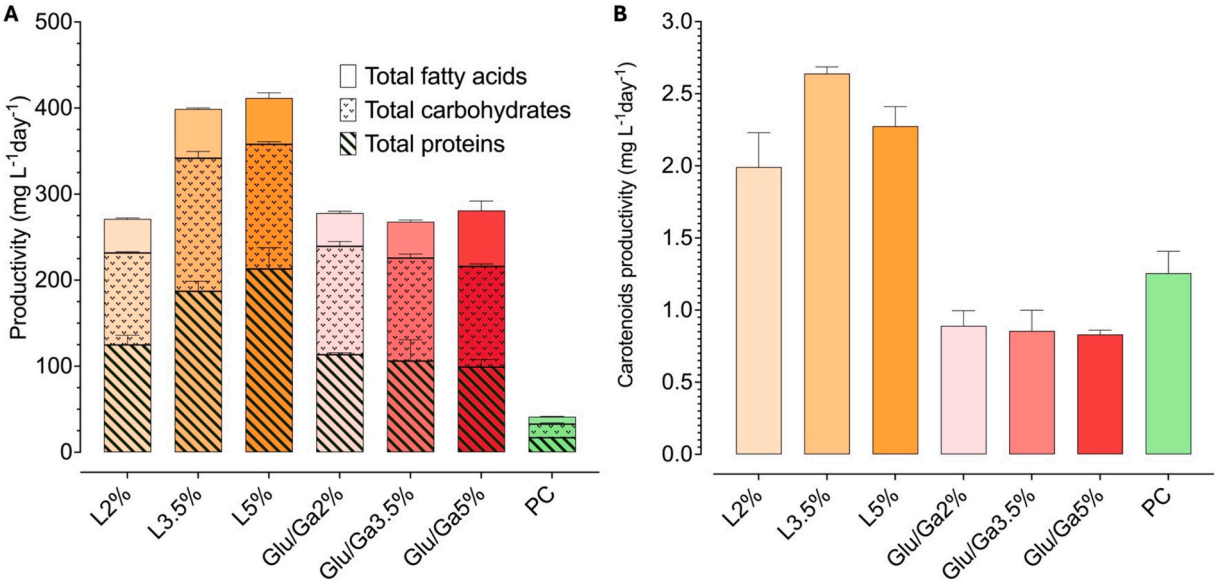

Fig. 4. Macromolecular productivity under lactose (L2 %, L3.5 %, L5 %), glucose/galactose (Glu/Ga2 %, Glu/Ga 3.5 %, Glu/Ga5 %) and photoautotrophic control (PC) conditions. (A) Total productivity of proteins, carbohydrates, and fatty acids (mg L^{-1} day^{-1}). Each bar represents the cumulative contribution of each macromolecular fraction for each treatment. (B) Carotenoid productivity (mg L^{-1} day^{-1}). Values are expressed as mean ± SD (n = 3).

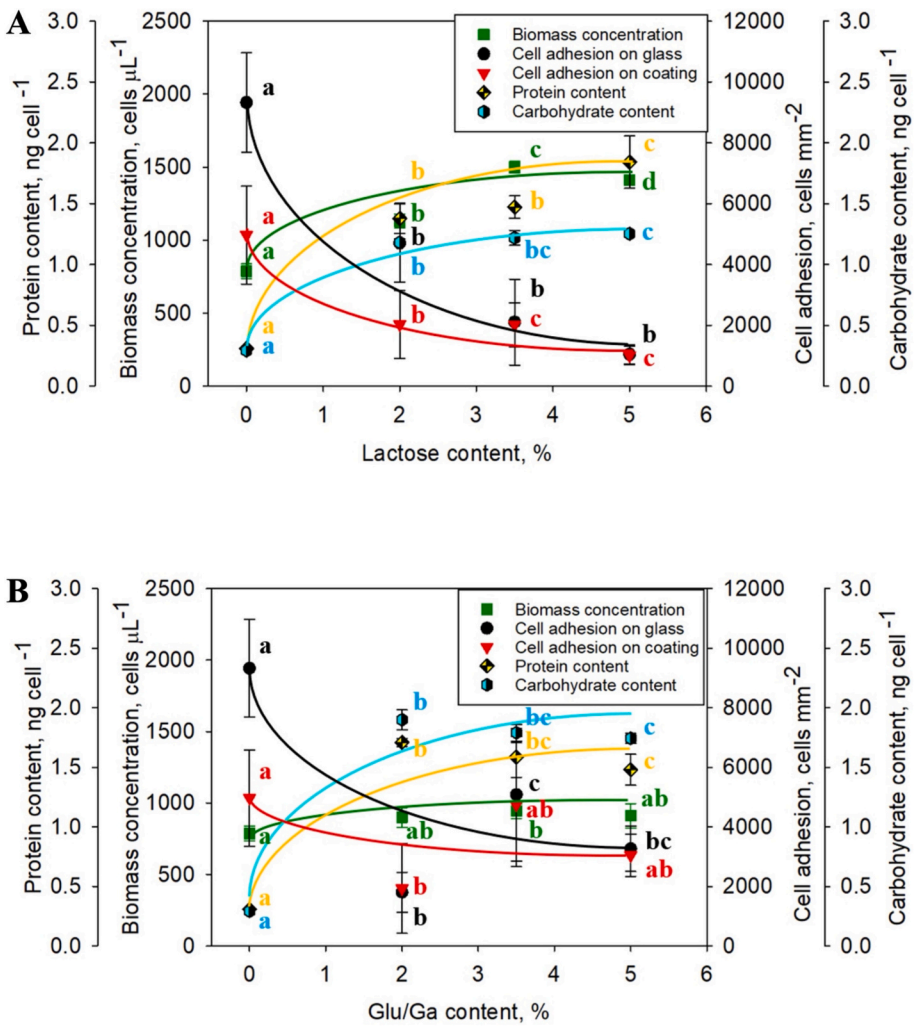

Fig. 5. Influence of (A) lactose content (%) and (B) Glu/Ga content (%) on biomass concentration, cell adhesion on the glass control and on the developed coating, as well as on the biomass composition. Note that the photoautotrophic cultures used as control are the 0 % in both cases. The lowercase letters represent significant differences with a p-value < 0.05. Solid lines connecting data points are shown to highlight the trend observed for each variable.

was directly assessed. Therefore, both algal enzymatic activity and the presence of associated microorganisms remain plausible explanations for the observed lactose-supported growth. In line with Apse et al. (2025), these observations further highlight the complexity of lactose- and whey-based cultivation systems. In the case of *T. chuii,* for which β-galactosidase activity has not been demonstrated to date (Kolesovs and Semjonovs, 2023; Cocksedge et al., 2025), the contribution of an associated microbiome may represent a plausible explanation for the observed lactose-supported response (Wang et al., 2016; Cabezudo et al., 2025). An alternative explanation is that the observed response reflects the different dynamics of carbon assimilation. Previous studies have suggested that a gradual release and utilization of organic carbon can favor the maintenance of physiological balance in mixotrophic microalgae (Sen and Martin, 2018; Silva et al., 2023; Proietti Tocca et al., 2024). Accordingly, lactose may have been metabolized more progressively than the glucose/galactose mixture, resulting in lower metabolic stress and a better preservation of photosynthetic functionality, thereby limiting the development of severe stress responses (Rafay et al., 2020; Sankhalkar et al., 2025). In line with this pattern, lactose-cultivated cells maintained photosynthetic activity throughout cultivation, with Fv/Fm values remaining between 0.40 and 0.50. In contrast, glucose/galactose treatments exhibited rapid photosynthetic collapse by day 4. These findings challenge the conventional view that mixotrophic growth necessarily leads to a functional downscaling of photosynthesis (Daneshvar et al., 2019; Calderini et al., 2022; Alkhamis and Qin, 2016; Arora and Philippidis, 2021; Boopathy et al., 2020)

Lactose-cultivated cells maintained near-neutral pH throughout cultivation, whereas glucose/galactose mixtures caused rapid acidification within 2 days of cultivation, requiring repeated NaOH (0.1 M) additions. This behaviour is typically observed when heterotrophic metabolism prevails over autotrophic carbon fixation, leading to CO_2 production by the microalgal cells themselves, or when readily available simple sugars rapidly stimulate the proliferation of associated bacteria and the production of organic acids (Arora et al., 2021; Li et al., 2022; Cao et al., 2023). The relatively stable pH observed in lactose cultures may be attributed to the slower utilization of lactose, which likely reduced the production of acidic metabolites, together with sustained photosynthetic activity that promoted net CO_2 fixation and consequent alkalinization of the medium through Calvin cycle-driven carbon assimilation. Furthermore, this pH stability was associated with maintained photosynthetic efficiency, suggesting a more stable physiological response under lactose-supported mixotrophy. Flow cytometry observations also supported the overall interpretation proposed above, confirming differences between treatments. Lactose populations exhibited a profile consistent with photosynthetically active cells, with a more homogeneous size profile, moderate side scatter, and preserved chlorophyll autofluorescence. In contrast, glucose/galactose populations showed predominantly smaller cells, elevated side scatter, and near-

baseline autofluorescence, indicating severe photosynthetic degradation and accumulation of storage compounds. FSC data showed a high number of particles falling outside the typical size range reported for *T. chuii* (Maulani et al., 2024), especially in the Glu/Ga treatments, suggesting high algal mortality and metabolic collapse.

4.2. Biomass composition under different carbon sources

Lactose-supported cultures exhibited a more balanced biochemical profile, combining protein accumulation with moderate pigment content. The marked protein increase relative to photoautotrophic controls agrees with previous reports on *T. chuii,* which suggest that mixotrophic cultivation can increase protein content by up to 3–4-fold, likely due to improved metabolic coordination between carbon and nitrogen assimilation under a more balanced physiological state (Conlon et al., 2024; Do et al., 2025). Notably, lactose-grown cultures showed high carotenoid productivity, particularly at 3.5 % (2.63 mg L^{-1} day^{-1}), as the more stable physiological state reached under these conditions preserved photosynthetic activity while supporting secondary metabolite production. It is important to consider that the same response may not necessarily be observed in real dairy matrices, whose greater compositional complexity may influence microalgal physiology differently. In fact, studies using cheese whey or scotta have reported increased biomass accumulation but, in some cases, lower pigment content or need for additional stress conditions to stimulate carotenoid synthesis, likely as a consequence of the more complex substrate matrix (Ribeiro et al., 2017; Salah et al., 2023). Conversely, glucose/galactose treatments exhibited the canonical mixotrophic stress response: reduced chlorophyll and carotenoid contents, with pronounced accumulation of carbohydrates and fatty acids, reflecting a storage-oriented metabolic response reported in other similar mixotrophic microalgal systems (Han et al., 2016; Boopathy, 2020). This corresponds to the "mixotrophy-to-heterotrophy shift", a metabolic transition in which cells progressively rely less on photosynthesis and more on organic carbon catabolism, with glycolysis becoming dominant and resources redirected toward carbon storage (Roth et al., 2017; Zhang et al., 2021; Perez Saura et al., 2025), thereby favoring the accumulation of reserve compounds while compromising biosynthetic and photosynthetic efficiency.

4.3. Relevance for dairy side-stream valorization and antifouling performance

The identification of 3.5 % lactose as optimal is directly relevant for dairy side-stream applications. Second cheese-whey and concentrated whey permeates contain approximately 4.0–6.0 % (w/v) lactose (Ozcelik et al., 2024; Sciuto et al., 2025), a concentration range fully compatible with that evaluated in this study. Importantly, the proposed cultivation strategy does not require preliminary lactose hydrolysis, thereby avoiding an additional enzymatic processing step that substantially increases operational costs and represents a major constraint to the economic feasibility of conventional lactose-based microalgal bioprocesses. The direct use of whey-derived lactose could therefore integrate microalgal cultivation into existing dairy processing workflows without additional upstream treatment, offering both economic and logistical advantages. Beyond growth and productivity, the performance of cultivation systems at pilot and industrial scales can be strongly affected by biofouling phenomena, especially in mixotrophic processes, where the presence of dissolved organic matter and extracellular polymeric substances can accelerate surface colonization and PBR fouling. In these systems, biofouling reduces light penetration, alters hydrodynamics, increases cleaning frequency, and compromises process productivity and operational costs (Zeriouh et al., 2017). For this reason, the antifouling behaviour of the PEG/PDMS coating was evaluated. The results confirm the robust antifouling performance of the PEG/PDMS surface previously reported (Garcia-Abad et al., 2022; Soriano-Jerez et al., 2024; Conlon and Touzet, 2025). A consistent reduction in cell adhesion was observed on the coated surface compared with glass, with adhesion levels remaining approximately 50 % lower across all tested treatments, irrespective of carbon source type and concentration, indicating that the antifouling effect remained stable under different metabolic conditions. To the best of our knowledge, this is among the first studies evaluating this type of coating under mixotrophic conditions. Despite the increased biological complexity associated with mixotrophic cultures, adhesion on the PEG/PDMS surface remained low and stable, supporting its potential application in intensified large-scale microalgal cultivation, including mixotrophic valorization systems.

Finally, the enhanced productivities achieved under lactose supplementation, together with the favorable protein-rich biomass composition and the positive performance of the PEG/PDMS coating, highlight the potential of this approach for future application-oriented developments. In particular, these findings support its prospective implementation in sustainable food and feed production systems, as well as in the valorization of lactose-rich dairy side streams.

5. Conclusion

This study, under the tested conditions, shows that lactose is a promising carbon source for the mixotrophic cultivation of *T. chuii* compared with glucose/galactose mixtures. At the optimal concentration of 3.5 % (w/v), lactose-supplemented cultures achieved higher cell densities, higher specific growth rates, and maintained photosynthetic competence throughout cultivation. Lactose cultivation also yielded a balanced biomass composition suitable for high-value applications, with the 3.5 % (w/v) condition maximizing carotenoid productivity and the 5 % (w/v) condition enhancing protein accumulation. In contrast, glucose/galactose supplementation promoted a physiological state resembling heterotrophic stress, characterized by the accumulation of storage metabolites, progressive impairment of the photosynthetic machinery, and increased cell death. Overall, the results suggest that lactose-rich dairy side streams, including second cheese whey and dairy wastewater, may represent promising substrates for the sustainable cultivation of *T. chuii* and their valorization through microalgal biorefinery approaches. The integration of PEG/PDMS coatings with mixotrophic cultivation may provide a promising approach for the development of transparent and low-biofouling surfaces in scalable microalgal biotechnological applications. Further studies are needed to validate these findings under real dairy wastewater conditions, investigate process scale-up, and evaluate the economic viability of the proposed strategy through detailed techno-economic assessments.

Supplementary Table S1 summarizes the maximum specific growth rate (μ), biomass productivity (PB), nitrate and phosphate removal percentages, and total carbohydrate (TC) reduction for each treatment. Supplementary Table S2 provides a comparative overview of the studies discussed in the text and highlights the specific novelty of the present study.

CRediT authorship contribution statement

Gloria Sciuto: Writing – original draft, Investigation, Formal analysis. **Salim Kichouh-Aiadi:** Writing – original draft, Investigation, Formal analysis. **Yolanda Soriano-Jerez:** Writing – original draft, Investigation, Formal analysis. **Cinzia L. Randazzo:** Writing – review & editing, Supervision, Data curation. **Nunziatina Russo:** Writing – review & editing, Methodology, Data curation. **Cinzia Caggia:** Writing – review & editing, Supervision, Resources, Project administration, Methodology, Funding acquisition, Conceptualization. **Maria del Carmen Cerón-García:** Project administration, Methodology, Funding acquisition, Conceptualization. **Asterio Sánchez-Mirón:** Writing – review & editing, Supervision, Project administration, Methodology, Funding acquisition, Conceptualization.

Funding

This study was partially funded by Italian PNRR, "SAMOTHRACE" – CUP E63C22000900006, n. CN00000022 – within Task 1: Sustainable management of water resources in agriculture (WP5-Spoke 1).

Declaration of competing interest

The authors declare that they have no known competing financial interests or personal relationships that could have appeared to influence the work reported in this paper.

Acknowledgement

The activities were performed within the Ph.D. program in Biotecnologie (XXXIX cycle) by Gloria Sciuto, granted by the PR Sicilia FSE + 2021-2027 n. 11/2023 A.A. 2023/2024, D.D.G. n. 3641 of 28/12/2023, at the University of Catania, in collaboration with the University of Almería, within projects funded by the Spanish Ministry of Economy and Competitiveness and the European Regional Development Fund (P_LANZ_2024/010; PPITUAL, Junta de Andalucía-FEDER 2021-2027-Program: 54.A; and Project PDC2022-133206- I100).

Appendix A. Supplementary data

Supplementary data to this article can be found online at https://doi.org/10.1016/j.biortech.2026.135339.

Data availability

Data will be made available on request.

References

Alkhamis, Y., Qin, J.G., 2016. Comparison of pigment and proximate compositions of *Tisochrysis lutea* in phototrophic and mixotrophic cultures. J. Appl. Phycol. 28, 35–42. https://doi.org/10.1007/s10811-015-0599-0.

de Andrade, A. F., e Silva, P. E. D. C., de Melo, R. G., do Nascimento Ferreira, M. P., Porto, A. L. F., Bezerra, R. P., 2022. Microalgal production under mixotrophic conditions using cheese whey as substrate. *Acta Sci. Biol. Sci.* 44, e62512. https://doi.org/10.4025/actascibiolsci.v44i1.62512.

Apse, O.J., Neiberts, K., Sukaruka, S., Tumpelis, T., Semjonovs, P., 2025. Valorisation of whey by mixotrophic and heterotrophic cultivation of microalgae for biomass and lipid production. Biodegradation 36, 106. https://doi.org/10.1007/s10532-025-10203-8.

Arora, N., Philippidis, G.P., 2021. Insights into the physiology of *Chlorella vulgaris* cultivated in sweet sorghum bagasse hydrolysate for sustainable algal biomass and lipid production. Sci. Rep. 11, 6779. https://doi.org/10.1038/s41598-021-86372-2.

Bhatnagar, A., Chinnasamy, S., Singh, M., Das, K.C., 2011. Renewable biomass production by mixotrophic algae in the presence of various carbon sources and wastewaters. Appl. Energy 88, 3425–3431. https://doi.org/10.1016/j.apenergy.2010.12.064.

Boopathy, A.B., Jayakumar, T., Chinnasamy, S., Rajaram, M.G., Mohan, N., Nagaraj, S., Chang, C.C., 2020. Biomass and lipid production potential of an Indian marine algal isolate *Tetraselmis striata* BBRR1. Energies 13, 341.https://doi.org/10.3390/en13020341.

Buchanan, D., Martindale, W., Romeih, E., Hebishy, E., 2023. Recent advances in whey processing and valorisation: Technological and environmental perspectives. Int. J. Dairy Technol. 76, 291–312. https://doi.org/10.1111/1471-0307.12935.

Cabezudo, R.G., Castro, J.C., Castro, C.G., Rodríguez, H.N., García, G.L., Vizcarra, P.M., 2025. Bioremediation potential of a non-axenic cyanobacterium *Synechococcus* sp. for municipal wastewater treatment in the Peruvian Amazon. Biotech 14, 36. https://doi.org/10.3390/biotech14020036.

Calderini, M.L., Salmi, P., Rigaud, C., Peltomaa, E., Taipale, S.J., 2022. Metabolic plasticity of mixotrophic algae is key for their persistence in browning environments. Mol. Ecol. 31, 4726–4738. https://doi.org/10.1111/mec.16619.

Camacho-Rodríguez, J., Cerón-García, M.C., Fernández-Sevilla, J.M., Molina-Grima, E., 2015. Genetic algorithm for the medium optimization of the microalga *Nannochloropsis gaditana* cultured for aquaculture. Bioresour. Technol. 177, 102–109. https://doi.org/10.1016/j.biortech.2014.11.057.

Cao, Y., Yang, S., Wang, J., Kong, W., Guo, B., Xi, Y., 2023. Metabolomic exploration of the physiological regulatory mechanisms of *Chlorella vulgaris* under different trophic conditions. Biomass Bioenergy 173, 106775. https://doi.org/10.1016/j.biombioe.2023.106775.

Casagli, F., Rossi, S., Steyer, J.P., Bernard, O., Ficara, E., 2021. Balancing microalgae and nitrifiers for wastewater treatment. Environ. Sci. Technol. 55, 3940–3955. https://doi.org/10.1021/acs.est.0c05264.

Cerón-García, M.C., González-López, C.V., Camacho-Rodríguez, J., López-Rosales, L., García-Camacho, F., Molina-Grima, E., 2018. Maximizing carotenoid extraction from microalgae. Food Chem. 257, 316–324. https://doi.org/10.1016/j.foodchem.2018.02.154.

Choi, H.J., 2016. Dairy wastewater treatment using microalgae for potential biodiesel application. Environ. Eng. Res. 21, 393–400. https://doi.org/10.4491/eer.2015.151.

Cocksedge, S.P., Mantecón, L., Castaño, E., Infante, C., Bailey, S.J., 2025. The potential of superoxide dismutase-rich *Tetraselmis chuii* as a promoter of cellular health. Int. J. Mol. Sci. 26, 1693. https://doi.org/10.3390/ijms26041693.

Conlon, T., Aranyos, A., Luck, T., Touzet, N., 2024. Effects of trophic mode and medium composition on *Tetraselmis chuii*. Biocatal. Agric. Biotechnol. 61, 103362. https://doi.org/10.1016/j.bcab.2024.103362.

Conlon, T., Touzet, N., 2025. Bioactive metabolites and extracellular vesicles from the marine chlorophyte genus *Tetraselmis*. Biotechnol. Adv. 108662. https://doi.org/10.1016/j.biotechadv.2025.108662.

Daneshvar, E., Zarrinmehr, M.J., Koutra, E., Kornaros, M., Farhadian, O., Bhatnagar, A., 2019. Sequential cultivation of microalgae in raw and recycled dairy wastewater. Bioresour. Technol. 273, 556–564. https://doi.org/10.1016/j.biortech.2018.11.059.

Das, P.K., Rani, J., Rawat, S., Kumar, S., 2022. Microalgal co-cultivation for biofuel production and bioremediation. Bioenergy Res. 15, 1–26. https://doi.org/10.1007/s12155-021-10254-8.

do Amaral Santos, M. J. B., de Souza Andrade, D., Bosso, A., Murata, M. M., Morioka, L. R. I., da Silva, J. B., Suguimoto, H. H., 2021. *Chlorella sorokiniana* cultivation in cheese whey for β-galactosidase production. *Res. Soc. Dev.* 10, e468101220727.

Do, J.M., Yeo, H.T., Suh, H.S., Seo, Y.H., Choi, H.N., Park, S.B., Yoon, H.S., 2025. Effect of salinity stress on *Coelastrella* sp. Biofuels 1–11. https://doi.org/10.1080/17597269.2025.2456400.

Garcia-Abad, L., López-Rosales, L., Cerón-García, M.D.C., Fernández-García, M., García-Camacho, F., Molina-Grima, E., 2022. Influence of abiotic conditions on biofouling formation in microalgal cultures. Biofouling 38, 507–520. https://doi.org/10.1080/08927014.2022.2089564.

Gondi, R., Kavitha, S., Kannah, R.Y., Karthikeyan, O.P., Kumar, G., Tyagi, V.K., Banu, J. R., 2022. Algal-based systems for removal of emerging pollutants from wastewater. Bioresour. Technol. 344, 126245. https://doi.org/10.1016/j.biortech.2021.126245.

Han, J., Zhang, L., Wang, S., Yang, G., Zhao, L., Pan, K., 2016. Co-culturing bacteria and microalgae in organic carbon-containing medium. J. Biol. Res. (thessalon.) 23, 8. https://doi.org/10.1186/s40709-016-0047-6.

Heifetz, P.B., Forster, B., Osmond, C.B., Giles, L.J., Boynton, J.E., 2000. Effects of acetate on facultative autotrophy in *Chlamydomonas reinhardtii*. Plant Physiol. 122, 1439–1446. https://doi.org/10.1104/pp.122.4.1439.

Hidasi, N., Badary, A., Jenkins, H.D., Fields, F.J., Mayfield, S.P., Ferrari, S., 2024. Selection and characterization of a *Parachlorella kessleri* microalgal strain able to assimilate lactose, and grow on dairy waste. Biomass Bioenergy 188, 107344. https://doi.org/10.1016/j.biombioe.2024.107344.

Hosseini, H., Saadaoui, I., Cherif, M., Siddiqui, S.A., Sayadi, S., 2022. Wastewater treatment using photobioreactors for *Tetraselmis* sp. Environ. Sci. Pollut. Res. 29, 61905–61937. https://doi.org/10.1016/j.biortech.2023.129991.

Hyung, J.H., Kim, E.J., Moon, S.J., Kang, N.S., Park, J., 2021. Tetraselmis Jejuensis Sp. Nov. Plants 10, 1289. https://doi.org/10.3390/plants10071289.

Kiani, H., Azimi, Y., Li, Y., Mousavi, M., Cara, F., Mulcahy, S., Halim, R., 2023. Nitrogen and phosphate removal from dairy processing side-streams by monocultures or consortium of microalgae. J. Biotechnol. 361, 1–11.

Kichouh-Aiadi, S., Gallardo-Rodríguez, J.J., Cerón-García, M.C., López-Rosales, L., García-Camacho, F., Sánchez-Mirón, A., 2025. Effects of hormones on *Amphidinium carterae*. Algal Res. 85, 103810. https://doi.org/10.1016/j.algal.2024.103810.

Kolesovs, S., Shvirksts, K., Grube, M., Vigants, A., 2025. Studies on lactose utilization by the microalga *Graesiella emersonii* in the 3N-BBM-V model medium. Eur. J. Phycol. 60, 175–184. https://doi.org/10.1080/09670262.2025.2471784.

Kolesovs, S., Semjonovs, P., 2023. Microalgal conversion of whey and lactose substrates. Biodegradation 34, 405–416. https://doi.org/10.1007/s10532-023-10033-6.

La Bella, E., Occhipinti, P.S., Puglisi, I., Fragalà, F., Saccone, R., Russo, N., Randazzo, C. L., Caggia, C., Baglieri, A., 2023. Comparative Phycoremediation Performance of Microalgae. Sustainability 15, 11644. https://doi.org/10.3390/su151511644.

Levasseur, M., Thompson, P.A., Harrison, P.J., 1993. Physiological acclimation of marine phytoplankton to different nitrogen sources. J. Phycol. 29, 587–595. https://doi.org/10.1111/j.0022-3646.1993.00587.

Li, T., Pang, N., He, L., Xu, Y., Fu, X., Tang, Y., Chen, S., 2022. Reprogramming glucose catabolism in *Chlorella sorokiniana*. Biomolecules 12, 939. https://doi.org/10.3390/biom12070939.

Lu, L., Wang, J., Yang, G., Zhu, B., Pan, K., 2017. Biomass and nutrient productivities of *Tetraselmis chuii* under mixotrophic conditions. Chin. J. Oceanol. Limnol. 35, 303–312. https://doi.org/10.1007/s00343-016-5299-3.

Macedo, A., Duarte, E., Fragoso, R., 2015. Ultrafiltration membranes for ovine second cheese whey fractionation. Int. Dairy J. 48, 31–37. https://doi.org/10.1016/j.idairyj.2014.12.003.

Mahdavi, S., Tavakoli, O., 2025. Co-cultivation of *Tetraselmis chuii* and *Chlorella vulgaris* in dairy wastewater. J. Water Process Eng. 73, 107572. https://doi.org/10.1016/j.jwpe.2025.107572.

Malavasi, V., Soru, S., Cao, G., 2020. Extremophile microalgae: Biotechnological potential. J. Phycol. 56, 559–573. https://doi.org/10.1111/jpy.12965.

Mercado, I., Álvarez, X., Verduga, M.E., Cruz, A., 2020. Enhancement of biomass and lipid productivity of *Scenedesmus* sp. Processes 8, 1458. https://doi.org/10.3390/pr8111458.

Majchrzak, M., Paterson, S., Gutiérrez-Corral, J., Gómez-Garre, D., Ortega-Hernández, A., de la Fuente, M.Á., Gómez-Cortés, P., 2025. Modulatory effects of *Tetraselmis chuii* gastrointestinal digests. Foods 14, 2106. https://doi.org/10.3390/foods14122106.

Maulani, Y.N., Swasta, I.B.J., Permana, G.N., Sujarwani, S., 2024. Effect of using different culture media on the growth of phytoplankton *Tetraselmis chuii*. Adv. Trop. Biodivers. Environ. Sci. 8, 26–32. https://doi.org/10.1016/j.chemosphere.2024.142868.

Minio, M., Battistuzzi, M., Norici, A., La Rocca, N., Pagliano, C., Gerotto, C., 2025. Effects of sulfate limitation on photosynthesis and cell composition of unicellular marine microalgae of different phylogenies. Physiol. Plant. 177, e70401. https://doi.org/10.1111/ppl.70401.

Muller-Feuga, A., Robert, R., Cahu, C., Robin, J., Divanach, P., 2003. Uses of microalgae in aquaculture. Live Feeds Mar. Aquac. 253–299. https://doi.org/10.1002/9780470995143.ch7.

Nzayisenga, J.C., Eriksson, K., Sellstedt, A., 2018. Mixotrophic and heterotrophic lipid production using wastewater. Bioresour. Technol. 257, 260–265. https://doi.org/10.1016/j.biortech.2018.02.085.

Occhipinti, P.S., Del Signore, F., Canziani, S., Caggia, C., Mezzanotte, V., Ferrer-Ledo, N., 2023. Mixotrophic and heterotrophic growth of *Galdieria sulphuraria* using buttermilk as a carbon source. J. Appl. Phycol. 35, 2631–2634. https://doi.org/10.1007/s10811-023-03012-0.

Occhipinti, P.S., Russo, N., Foti, P., Pino, A., Randazzo, C.L., Pollio, A., Caggia, C., 2025. Microalgal pool for *Escherichia coli* removal. J. Sci. Food Agric. 105, 1288–1297. https://doi.org/10.1002/jsfa.13918.

Omran, B.A., Baek, K.H., 2022. Agro-industrial biowaste valorization for wastewater treatment. J. Environ. Manage. 311, 114806. https://doi.org/10.1016/j.jenvman.2022.114806.

Ozcelik, D., Suwal, S., Ray, C., Tiwari, B.K., Jensen, P.E., Poojary, M.M., 2024. Valorization of dairy side-streams for microalgal cultivation. Trends Food Sci. Technol. 146, 104386. https://doi.org/10.1016/j.tifs.2024.104386.

Pereira, M.I., Chagas, B.M., Sassi, R., Medeiros, G.F., Aguiar, E.M., Borba, L.H., Rangel, A.H., 2019. Mixotrophic cultivation of *Spirulina platensis* in dairy wastewater. PLoS One 14, e0224294. https://doi.org/10.1371/journal.pone.0224294.

Perez Saura, P., Cardol, P., Remacle, C., 2025. Xylose assimilation in *Auxenochlorella protothecoides*. J. Appl. Phycol. 1–13. https://doi.org/10.1007/s10811-025-03585-y.

Pires, A.F., Marnotes, N.G., Rubio, O.D., Garcia, A.C., Pereira, C.D., 2021. A review on the valorization of whey. Foods 10, 1067. https://doi.org/10.3390/foods10051067.

Prazeres, A.R., Carvalho, F., Rivas, J., 2012. Cheese whey management. J. Environ. Manage. 110, 48–68. https://doi.org/10.1016/j.jenvman.2012.05.018.

Proietti Tocca, G., Agostino, V., Menin, B., Tommasi, T., Fino, D., Di Caprio, F., 2024. Mixotrophic and heterotrophic growth using acetate. Rev. Environ. Sci. Biotechnol. 23, 93–132. https://doi.org/10.1007/s11157-024-09682-7.

Rafay, R., Uratani, J.M., Hernández, H.H., Rodríguez, J., 2020. Growth and nitrate uptake in batch reactors. Front. Mar. Sci. 7, 77. https://doi.org/10.3389/fmars.2020.00077.

Rahman, N.A., Khatoon, H., Yusuf, N., Banerjee, S., Haris, N.A., Lananan, F., Tomoyo, K., 2017. *Tetraselmis chuii* biomass as shrimp feed additive. Int. Aquat. Res, 9, 235–247. https://doi.org/10.1007/s40071-017-0173-2.

Ribeiro, J.E., Martini, M., Altomonte, I., Salari, F., Nardoni, S., Sorce, C., Silva, F., Andreucci, A., 2017. Production of *Chlorella protothecoides* biomass, chlorophyll and carotenoids using the dairy industry by-product scotta as a substrate. Biocatal. Agric. Biotechnol. 11, 207–213. https://doi.org/10.1016/j.bcab.2017.07.007.

Rodríguez-Ruiz, J., Belarbi, E.H., Sánchez, J.L.G., Alonso, D.L., 1998. Rapid lipid extraction and transesterification. Biotechnol. Tech. 12, 689–691. https://doi.org/10.1023/A:1008812904017.

Roth, M.S., Cokus, S.J., Gallaher, S.D., Walter, A., Lopez, D., Erickson, E., Niyogi, K.K., 2017. Genome assembly of *Chromochloris zofingiensis*. PNAS 114, E4296–E4305. https://doi.org/10.1073/pnas.1619928114.

Ryan, M.P., Walsh, G., 2016. The biotechnological potential of whey. Rev. Environ. Sci. Biotechnol. 15, 479–498. https://doi.org/10.1007/s11157-016-9402-1.

Salah, A., Sany, H., El-Sayed, A.E.K.B., El-Bahbohy, R.M., Mohamed, H.I., Amin, A., 2023. Growth performance and biochemical composition of *Desmodesmus* sp. green alga grown on agricultural industries waste (cheese whey). Water Air Soil Pollut. 234, 770. https://doi.org/10.1007/s11270-023-06780-0.

Sánchez-Zurano, A., Villaró-Cos, S., Ciardi, M., Acién-Fernández, F.G., Fernández-Sevilla, J.M., Lafarga, T., 2024. Mixotrophic production of *Chlorella vulgaris* using whey. J. Appl. Phycol. 36, 87–100. https://doi.org/10.1007/s10811-023-03142-5.

Sankhalkar, S., Jamuni, V., Pai, R., 2025. Photosynthetic acclimation response of *Chlamydomonas reinhardtii* in synthetic dairy wastewater. J. Appl. Phycol. 1–12. https://doi.org/10.1007/s10811-025-03525-w.

Sial, A., Zhang, B., Zhang, A., Liu, K., Imtiaz, S.A., Yashir, N., 2021. Microalgal–bacterial synergistic interactions. Bioenergy Res. 14, 723–738. https://doi.org/10.1007/s12155-020-10213-9.

Sciuto, G., Russo, N., Randazzo, C.L., Caggia, C., 2025. Valorization of second cheese whey through microalgae. Biotech 14, 79. https://doi.org/10.3390/biotech14040079.

Sen, R., Martin, G.J., 2018. Glycerol and nitrate utilization by marine microalgae. Algal Res. 33, 298–309. https://doi.org/10.1016/j.algal.2018.06.002.

Shahid, A., Malik, S., Zhu, H., Xu, J., Nawaz, M.Z., Nawaz, S., Mehmood, M.A., 2020. Cultivating microalgae in wastewater for biomass production, pollutant removal, and atmospheric carbon mitigation: a review. Sci. Total Environ. 704, 135303. https://doi.org/10.1016/j.scitotenv.2019.135303.

Silva, S.C., Dias, M.M., Barreiro, M.F., 2023. What is next in microalgae research. Microalgae-Based Syst. Ch. 8. https://doi.org/10.1515/9783110781267-006.

Sim, S.J., Snell, K.D., Hogan, S.A., Stubbe, J., Rha, C., Sinskey, A.J., 1997. PHA synthase activity control. Nat. Biotechnol. 15, 63–67. https://doi.org/10.1038/nbt0197-63.

Soriano-Jerez, Y., Gourlaouen, E., Zeriouh, O., del Carmen Cerón-García, M., Arrabal-Campos, F.M., Ruiz-Martínez, C., Bressy, C., 2024. Role of dynamic surface tension of silicone polyether surfactant-based silicone coatings on protein adsorption: an insight on the 'ambiguous' interfacial properties of Fouling Release Coatings. Prog. Org. Coat. 186, 108079. https://doi.org/10.1016/j.porgcoat.2023.108079.

Soriano-Jerez, Y., López-Rosales, L., Cerón-García, M., Sánchez-Mirón, A., Gallardo-Rodríguez, J.J., García-Camacho, F., Molina-Grima, E., 2021. Long-term biofouling formation in *Nannochloropsis gaditana*. Biotechnol. Bioeng. 118, 1152–1165. https://doi.org/10.22541/au.159863446.65595547.

Villar-Navarro, E., Ruiz, J., Garrido-Pérez, C., Perales, J.A., 2022. Microalgae biotechnology for aquaculture. J. Water Process Eng. 49, 103115. https://doi.org/10.1016/j.jwpe.2022.103115.

Wang, Y., Zhang, C.H., Lin, M.M., Ge, Y., 2016. Arsenate absorption in *Dunaliella salina*. J. Hazard. Mater. 318, 443–451. https://doi.org/10.1016/j.jhazmat.2016.07.031.

Zeriouh, O., Reinoso-Moreno, J. V., López-Rosales, L., Cerón-García, M. del C., Sánchez-Mirón, A., García-Camacho, F., Molina-Grima, E., 2017. Biofouling in photobioreactors for marine microalgae. *Crit. Rev. Biotechnol.* 37, 10061023. https://doi.org/10.1080/07388551.2017.129961.

Zhang, Z., Sun, D., Cheng, K.W., Chen, F., 2021. Carbon and energy metabolism of mixotrophy. Biotechnol. Biofuels 14, 36. https://doi.org/10.1186/s13068-021-01890-5.

Zhao, K., Wu, Y.W., Young, S., Chen, X.J., 2020. Biological treatment of dairy wastewater. J. Environ. Inform. Lett. 4, 22–31. https://doi.org/10.3808/jeil.202000036.

Zhu, C.J., Lee, Y.K., 1997. Determination of biomass dry weight of marine microalgae. J. Appl. Phycol. 9, 189–194. https://doi.org/10.1023/A:1007914806640.